Level-Sets fields, placement and velocity based formulations of contact-impact problems

Hachmi Ben Dhia, Chokri Zammali

Level-Sets fields, placement and velocity based formulations of contact-impact problems

Hachmi Ben Dhia*,† and Chokri Zammali

Laboratoire MSS-Mat, Unité Mixte de Recherche 8579 CNRS, Ecole Centrale Paris,

Châtenay-Malabry 92295 cedex, France

By introducing unknown *Sign*-like fields of *Level-Sets* type, the *Signorini-Moreau* dynamic contact conditions are set merely as boundary equations. From this setting, a continuous hybrid weak–strong formulation for dynamic contact between deformable solids is derived and a new Lagrangian formulation (we call stabilized) generalizing both the classical and augmented ones is obtained. Friction phenomena are treated similarly. In the global problem, the irregular *Sign*-like fields stand for the intrinsic contact unknown ones. This problem is discretized by means of time, space and collocation schemes. Some numerical experimentations are carried out, showing the potential of our developments.

KEY WORDS: *Level-Sets*; contact; impact; *stabilized* Lagrangian formulation

1. INTRODUCTION

The effective contact zone is an intrinsic geometrical additional unknown in mechanical problems involving unilateral contact conditions when compared to the situation where classical (normal) transmission conditions are substituted to the latters. In this paper, this geometrical unknown quantity is lifted up by means of an unknown *Sign*-like field of *Level-Sets* type [1], defined on the assumed to be known potential contact surface. This Sign-like field plays a major part in our formulation of contact problems. Its *iso-1* values define the effective contact zone. This allows us to:

- write the classical Signorini conditions merely as standard boundary conditions defined on a known surface, namely the potential contact surface,

*Correspondence to: Hachmi Ben Dhia, Laboratoire MSS-Mat, Unité Mixte de Recherche 8579 CNRS, École Centrale Paris, Châtenay-Malabry 92295 cedex, France.

†E-mail: hachmi.ben-dhia@ecp.fr

- obtain quite naturally continuous hybrid weak formulation of contact problems of Lagrangian type (e.g. [2–7]),
- derive a *stabilized* Lagrangian formulation of contact problems extending both the classical and the augmented Lagrangian formulations [2, 5, 8–11] (see also the two monographs [12, 13] and the references therein),
- work out the problem with only fields as unknowns, defined either in the domains of the contacting solids (displacement and/or velocity fields) or on the potential contact surface (contact pressure and a *Level-Set* like field).
- use appropriate discretization numerical tools for the approximation of the continuous problem.

The same holds when friction phenomena are taken into account. In this situation, the additional intrinsic unknown field is the geometrical sub-zone of sticking points in the effective contact zone. An additional *Level-Set* unknown field whose *iso-1* values define the sticking zone in the effective contact zone is introduced.

When considering dynamic contact problems based on classical Signorini contact models, it is experienced that time discretization by classical schemes of these problems leads to oscillations of the discrete mechanical fields. Many remedies have been designed to tackle this pathology (e.g. [14–17]. More recently and by following Simo *et al.* [18] and using energy and momentum conservation arguments, the so-called persistent contact condition has been added by several authors to the Signorini contact displacement based conditions (e.g. [19–23]).

In this paper we use the formalism introduced by Moreau [24, 25] (see also Jean [26]) to write dynamic unilateral contact conditions. The Moreau dynamic contact model which controls both the relative normal placements of the contact interfaces and their respective normal velocities is here written in terms of equations, in the vein of what was performed in the field of Mathematical Programming for the development of robust algorithms (see e.g. Christensen and Klarbring [27] and the references therein). In these equations, two unknown *Level-Sets* fields are introduced to characterize dynamically the effective contact-impact zone. A continuous hybrid weak–strong *Level-Sets* and velocity based formulation is then easily derived. A stabilization of this formulation, generalizing both the Lagrangian and augmented-Lagrangian ones is suggested. The numerical approximation by means of a finite difference scheme, compatible mixed finite elements and a collocation method is developed. A simple numerical solution strategy, based on fixed points and generalized Newton methods is briefly described.

An outline of the paper is the following. Section 2 is devoted to the introduction of the mechanical contact problem and to the formulation of the virtual work principle for two bodies coming dynamically into contact in a large transformation framework. To define contact loads, dynamic contact laws are developed in Section 3. More precisely, the classical Signorini contact model is recalled in Section 3.1. Its proved to be equivalent formulations, using a *Level-Set* field whose *iso-1* values define the effective contact zone, are detailed in Section 3.2. What can be called the *Signorini-Moreau* unilateral dynamic contact model is recalled in Section 3.3 and its *Level-Sets* based equivalent setting is given in Section 3.4. Our *Level-Sets*, placement and velocity based weak–strong Lagrangian formulation of the dynamic contact problem is then derived in the frictionless case in Section 4.1. It is extended to take into account friction phenomena in Section 4.2. The stabilization of these formulations is discussed. A global solution strategy is detailed in Section 5: the time discretization scheme is described in Section 5.1 and an overview of the used spatial disretization methods, namely the finite element and the collocation methods, are presented in Section 5.2. The section is ended with a brief description of the numerical algorithm used to

solve the discrete non-linear and irregular obtained systems. The potential of our developments is demonstrated by rather classical and simple but significant contact and impact tests in Section 6.

2. THE VIRTUAL WORK PRINCIPLE

The virtual work principle (VWP) is here formulated for a system of two solids that may come dynamically into contact with each other in the large transformations framework. As classically done (e.g. [3]), the action and reaction principle is extended to the potential contact interface by means of pairing mappings that are defined. The behaviour law of the constitutive materials and the initial conditions are precised.

2.1. Notations and problem definition

We consider the problem of dynamic contact between two deformable solids S^1 and S^2 occupying the closures of the domains Ω_0^1 and Ω_0^2 of R^d, $(d = 2, 3)$ in their reference respective configurations and the closures of Ω_t^1 and Ω_t^2 of R^d in their current ones (see Figure 1). The deformation (or motion) $\boldsymbol{\varphi}^i$ of the solid S^i is an application (assumed to be sufficiently regular in space and time, except may be at isolated instants), defined as following:

$$\begin{aligned} \boldsymbol{\varphi}^i &: \Omega_0^i \times \mathrm{I} \longrightarrow \Omega_t^i \\ &(\mathbf{p}^i, t) \longmapsto \mathbf{x}^i(t) \end{aligned} \tag{1}$$

with $\mathrm{I} = [t_0, t_f]$ standing for the time interval of study of the mechanical problem.

The space R^d is supposed to be endowed with an orthonormal basis $(\mathbf{e}_1, \ldots, \mathbf{e}_d)$.

It is assumed that in their initial configurations, the two solids are not in contact and are free of residual stresses. The boundary of each Ω_0^i is partitioned into Γ_u^i, the part on which the displacements are prescribed, Γ_g^i the one on which the surface loads are given and Γ_c^i the final part on which contact may occur. The current positions of these boundary parts, assumed to constitute

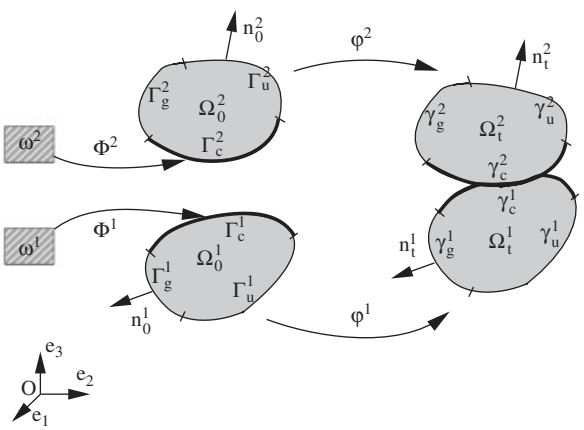

Figure 1. The contact problem.

a partition of the boundary of Ω_t^i, are denoted by γ_u^i, γ_g^i and γ_c^i, respectively. Moreover, the potential contact surfaces are assumed to be parameterized *via* two regular mappings, denoted by Φ^i and defined from given domains ω^i included in R^{d-1} into R^d (see Figure 1). The classical outward unit normals to the boundaries of the solids S^i are denoted by $\mathbf{n}_0^i$ and $\mathbf{n}_t^i$ in the reference and the current configurations, respectively. Notice here that finite element discretizations combined with large displacements lead generally only to piece-wise smooth deformed contact interfaces. This relevant numerical contact issue is not addressed in this paper. Some comments and references are however given in Section 5.2.

2.2. Virtual work principle

For clarity and without restriction, we consider here the case where the solids are clamped on Γ_u^i. Moreover, we assume that the applied surface loads are equal to zero on γ_g^i and neglect the body forces. The VWP reads then for each time $t \in \mathrm{I}$:

Find $\mathbf{u} = (\mathbf{u}^1, \mathbf{u}^2) \in \mathbf{CA}_u = \mathbf{CA}_u^1 \times \mathbf{CA}_u^2$; $\forall \mathbf{w} = (\mathbf{w}^1, \mathbf{w}^2) \in \mathbf{CA}_u$

$$\sum_{i=1}^{2} \int_{\Omega_0^i} \rho_0^i \ddot{\mathbf{u}}^i . \mathbf{w}^i \, \mathrm{d}\Omega_0^i + \sum_{i=1}^{2} \int_{\Omega_0^i} \mathrm{Tr}[\mathbf{\Pi}^i(\mathbf{u}^i)(\nabla_p(\mathbf{w}^i))^{\mathrm{T}}] \, \mathrm{d}\Omega_0^i - \int_{\Gamma_c} \mathbf{R}.[\![\mathbf{w}]\!] \, \mathrm{d}\Gamma_p = 0 \tag{2}$$

In system (2), $\mathbf{CA}_u^i$, $i = 1, 2$, denotes the space of kinematically admissible fields, $\mathbf{u}^i$ and $\ddot{\mathbf{u}}^i$ are the displacement and acceleration fields, Γ_c $(= \Gamma_c^1)$ is the potential contact 'slave' surface, ρ_0^i denotes the mass density in the reference state of solid S^i and $\mathbf{\Pi}^i$ is the first Piola–Kirchhoff stress tensor defined in Ω_0^i. The nominal vector-valued unknown density of contact forces is denoted by $\mathbf{R}$ $(= \mathbf{R}^1)$. This density of forces is experienced by solid S^1 from solid S^2. Moreover, the action and reaction principle is used. In the present context, this principle is extended as following:

$$\mathbf{R}^1(\mathbf{p}, t) = -\mathbf{R}^2(\overline{\mathbf{p}}(t), t) \quad \text{for } (\mathbf{p}, t) \in \Gamma_c \times \mathrm{I} \tag{3}$$

where $\overline{\mathbf{p}}(t)$ is, for each $t \in \mathrm{I}$, a point belonging to the 'master' reference surface Γ_c^2, paired with the point $\mathbf{p}$ of Γ_c $(= \Gamma_c^1)$ by coupling-like applications of proximity type [28], or, more generally, by using any admissible direction along which the nearest point of Γ_c^2 to $\mathbf{p}$ is found [29]. Notice here that, at each time, the pairing application is defined from the evolving surface γ_c^1 into γ_c^2, then transported back to define a reference pairing application from Γ_c into Γ_c^2 by using the deformations $\boldsymbol{\varphi}^i$, for $i = 1, 2$, which in turn is transported to define the practically used pairing application from ω^1 into ω^2 thanks to the parameterizations Φ^i, for $i = 1, 2$.

With these pairing applications, a jump-like field is defined on Γ_c, at each time, as follows.

For each $\mathbf{w} = (\mathbf{w}^1, \mathbf{w}^2) \in \mathbf{CA}_u$,

$$[\![\mathbf{w}]\!](\mathbf{p}) = \mathbf{w}^1(\mathbf{p}) - \mathbf{w}^2(\overline{\mathbf{p}}(t)) \quad \text{for } (\mathbf{p}, t) \in \Gamma_c \times \mathrm{I} \tag{4}$$

This field is used in (2).

System (2) has now to be supplemented with material behaviour laws, initial conditions and contact laws. For this purpose, an hyperelastic behaviour is assumed (for clarity) for the constitutive materials of the considered solids. That is,

$$\mathbf{\Pi}^i = \rho_0^i \frac{\partial W^i}{\partial \mathbf{F}^i} \tag{5}$$

where W^i is a local internal elastic energy per mass unit and $\mathbf{F}^i$ is the deformation gradient tensor.

The initial conditions are the following:

$$\mathbf{u}^i(\mathbf{p}, t_0) = \mathbf{u}^{i0}, \quad \mathbf{v}^i(\mathbf{p}, t_0) = \mathbf{v}^{i0} \quad \text{for } \mathbf{p} \in \Omega_0^i \tag{6}$$

where $\mathbf{u}^{i0}$ and $\mathbf{v}^{i0}$ are given.

The contact actions constitute the subject of the following section.

3. DYNAMIC CONTACT LAWS

We denote by $\mathbf{n}$ the unit inward normal to the 'master' current surface transported back to the reference 'master' surface. More precisely,

$$\mathbf{n}(\mathbf{p}, t) = -\mathbf{n}_t^2(\varphi^2(\overline{\mathbf{p}}(t), t)) \quad \text{for } (\mathbf{p}, t) \in \Gamma_c \times \mathrm{I} \tag{7}$$

Now, using a classical decomposition of the nominal contact density of loads $\mathbf{R}$, we set:

$$\mathbf{R}(\mathbf{p}, t) = \lambda(\mathbf{p}, t)\mathbf{n}(\mathbf{p}, t) + \mathbf{R}_\tau(\mathbf{p}, t) \quad \text{for } (\mathbf{p}, t) \in \Gamma_c \times \mathrm{I} \tag{8}$$

where $\mathbf{R}_\tau$ refers to the density of tangential contact loads and λ is the normal contact pressure. These fields are defined by means of interface laws. Signorini and Coulomb's models are used in this paper and one of our key points is the equivalent setting of the latter in terms of equations in which *Sign*-like fields are introduced as intrinsic contact unknown fields.

3.1. The classical Signorini model

The classical displacement based Signorini contact conditions (known also as the Karuch–Kuhn–Tucker conditions) read:

$$d_n(\mathbf{p}, t) \leqslant 0 \quad \text{for } (\mathbf{p}, t) \in \Gamma_c \times \mathrm{I} \tag{9}$$

$$\lambda(\mathbf{p}, t) \leqslant 0 \quad \text{for } (\mathbf{p}, t) \in \Gamma_c \times \mathrm{I} \tag{10}$$

$$d_n(\mathbf{p}, t)\lambda(\mathbf{p}, t) = 0 \quad \text{for } (\mathbf{p}, t) \in \Gamma_c \times \mathrm{I} \tag{11}$$

where d_n denotes the signed distance defined by

$$d_n(\mathbf{p}, t) = (\varphi^1(\mathbf{p}, t) - \varphi^2(\overline{\mathbf{p}}(t), t)).\mathbf{n}(\mathbf{p}, t) \quad \text{for } (\mathbf{p}, t) \in \Gamma_c \times \mathrm{I} \tag{12}$$

3.2. A Level-Set based Signorini model

Denoting by $\Gamma_c^{\text{eff}}(t)$ the subset of points of Γ_c on which the contact is effective at a given time $t \in \mathrm{I}$, it is clear that the classical Signorini conditions can equivalently be written as

$$d_n = 0 \text{ and } \lambda \leqslant 0 \quad \text{on } \Gamma_c^{\text{eff}}(t) \quad \text{for } t \in \mathrm{I} \tag{13}$$

$$d_n < 0 \text{ and } \lambda = 0 \quad \text{on } \Gamma_c \backslash \Gamma_c^{\text{eff}}(t) \quad \text{for } t \in \mathrm{I} \tag{14}$$

By introducing a *Sign*-like field, as done in Ben Dhia [30] for a penalized unilateral contact model, the conditions above can equivalently be written as alternative of interface transmission conditions. Indeed, if we define:

$$S = 1_{R^-}(\lambda - \rho_n d_n) \quad \text{on } \Gamma_c \times \mathrm{I} \tag{15}$$

where ρ_n is a strictly positive user parameter, R^- is the semi-axis of negative reals and 1_K is the characteristic function of the set K ($1_K(x) = 1$ if $x \in K$ and 0 otherwise), then the local system (13) and (14) can be written as

$$S d_n = 0 \quad \text{on } \Gamma_c \times \mathrm{I} \tag{16}$$

$$(1 - S)\lambda = 0 \quad \text{on } \Gamma_c \times \mathrm{I} \tag{17}$$

Notice that the parameter ρ_n is in (15) homogeneous to a pressure divided by a length. Other user-like parameters will be introduced in the sequel. They obey to a similar homogeneity requirement.

Equation (16), both with the definition (15) of S, is an interface normal kinematic continuity condition on Γ_c^{eff}, whilst Equation (17) is a free static normal boundary condition that imposes $\lambda = 0$ on $\Gamma_c \backslash \Gamma_c^{\text{eff}}$. The unknown *Sign*-like field S can also be seen as a *Level-Set* field [1]; the unknown effective contact zone corresponding to the iso-1 *Level-Set*.

The fact that in our setting of the contact laws only equalities are involved is to be underlined. Another aspect intimately linked to the definition (15) of the *Level-Set* field S is that the (alternative)-interface conditions (16) and (17) can be gathered in only one interface equation. Indeed by introducing a homogenization user parameter $h_n \neq 0$, one can write the Signorini contact laws as follows:

$$S - 1_{R^-}(\lambda - \rho_n d_n) = 0 \quad \text{on } \Gamma_c \times \mathrm{I} \tag{18}$$

$$S d_n + \frac{(1 - S)}{h_n}\lambda = 0 \quad \text{on } \Gamma_c \times \mathrm{I} \tag{19}$$

Actually, the system defined by (15)–(17) is equivalent to the system defined by (18), (19). Indeed, the fact that (15)–(17) implies (18), (19) is obvious and the inverse is obtained easily by considering the two cases where the so-called augmented Lagrangian multiplier $g_n = \lambda - \rho_n d_n$ is in R^- or not. By analysing the same alternative for g_n, one can also easily check that the system (18), (19) implies the Signorini system, defined by (9)–(11). The fact that the Signorini system implies (15)–(17) is obtained by considering the alternative $d_n = 0$ and $\lambda = 0$ and checking easily that, defining S by (15), equalities (16) and (17) are fulfilled in either case.

In conclusion, we have proved that (9)–(11), (15)–(17) and (18), (19) are three equivalent settings of Signorini contact laws.

A straightforward weighted residual system can now be easily derived from (19) and a first global hybrid weak–strong continuous frictionless dynamic formulation of the contact problem can be obtained. However, it is well known that, due to shocks, the numerical fields which can be calculated by solving the latter by means of classical numerical schemes show spurious oscillations (see numerical section). More or less *a priori* or *a posteriori* physical based treatments have been designed by several authors to attenuate or kill these numerical oscillations (e.g. [14–16, 19, 20, 22, 31–33]). Here, by following the seminal ideas of Moreau [24–26], the

Signorini conditions are written in terms of relative normal placements and velocities of the contact surfaces.

3.3. The Signorini-Moreau model

Let us assume that at an initial time $t = t_0 \in \mathrm{I}$, the Signorini displacement based contact conditions are satisfied. That is,

$$d_n(\mathbf{p}, t_0) \leqslant 0 \quad \text{for } \mathbf{p} \in \Gamma_c \tag{20}$$

$$\lambda(\mathbf{p}, t_0) \leqslant 0 \quad \text{for } \mathbf{p} \in \Gamma_c \tag{21}$$

$$d_n(\mathbf{p}, t_0)\lambda(\mathbf{p}, t_0) = 0 \quad \text{for } \mathbf{p} \in \Gamma_c \tag{22}$$

The so-called 'viability lemma' of Moreau [24, 25, 34] asserts that with the hypotheses (20)–(22) and under some other reasonable ones (cf. Remark 1), the Signorini contact conditions (9)–(11) are satisfied at all future times as far as the following conditions are fulfilled:

For $(\mathbf{p}, t) \in \Gamma_c \times \mathrm{I}$

$$\text{if} \quad d_n(\mathbf{p}, t) < 0 \quad \text{then} \quad \lambda(\mathbf{p}, t) = 0 \tag{23}$$

otherwise

$$[\![v_n(\mathbf{p}, t)]\!] \leqslant 0 \tag{24}$$

$$\lambda(\mathbf{p}, t) \leqslant 0 \tag{25}$$

$$[\![v_n(\mathbf{p}, t)]\!]\lambda(\mathbf{p}, t) = 0 \tag{26}$$

where $[\![v_n]\!]$ stands for the normal velocity jump field in the sense of definition (4).

For the contact model, which is called here the *Signorini-Moreau* model, one can notice that both the relative normal placements and the relative normal velocities of the contact surfaces are controlled.

Remark 1
Rigorously speaking, the assumed to be defined right determination of the velocity fields (see e.g. [24, 26]) are to be used in (24) and (26) at shock instants.

3.4. Level-Sets based Signorini-Moreau model

By following the developments carried out in Section 3.2, we introduce now two *Sign*-like fields and write the *Signorini-Moreau* conditions as equations:

$$\lambda = S_u S_v(\lambda - h_n [\![v_n]\!]) \quad \text{on } \Gamma_c \times \mathrm{I} \tag{27}$$

$$S_u = 1_{R^-}(-d_n) \quad \text{on } \Gamma_c \times \mathrm{I} \tag{28}$$

$$S_v = 1_{R^-}(\lambda - \rho_n [\![v_n]\!]) \quad \text{on } \Gamma_c \times \mathrm{I} \tag{29}$$

where ρ_n is a strictly positive parameter and h_n is a non-zero parameter.

The dynamic contact problem will be formulated with this new equivalent setting of the *Signorini-Moreau* contact conditions in the following section. Notice that the equivalence between (23)–(26) and (27)–(29) can be proved by following similar lines to those developed in Section 3.2 for the proof of the equivalence between different formulations of the Signorini laws. It is not detailed here.

Remark 2
Another classical way of modelling dynamic contact loads consists in using regularized possibly damped or compliance models: (e.g. Oden and Martins [35])

$$\lambda = -k_n((d_n)^+)^{m_1} - c_n((d_n)^+)^{m_2}[\![v_n]\!] \tag{30}$$

where $(.)^+$ is the positive part of $(.)$ and where k_n, c_n, m_1 and m_2 are either numerical or material parameters characterizing the contact interface. Equation (30) can be treated weakly or strongly. In all cases, one can notice that an unknown *Sign*-like field can be defined by

$$S_p = 1_{R^-}(-d_n) \quad \text{on } \Gamma_c \times \mathrm{I} \tag{31}$$

as done in [30].

4. VELOCITY AND *LEVEL-SETS* BASED WEAK–STRONG FORMULATIONS

The frictionless formulation is given first. Then by using the equivalent formulation of the Coulomb's laws [36] (see also [6]) and by introducing an additional *Level-Set* field whose *iso-1* values define the sticking zone, a global dynamic and continuous weak–strong formulation taking into account friction loads is derived.

4.1. Frictionless Lagrangian formulations

By using the VWP (2) and operating a weak formulation of Equation (27) whilst keeping Equations (28) and (29) as local strong ones, the following weak–strong mixed formulation of the dynamic frictionless contact problem is obtained:

Assuming that the displacement and velocity fields $\mathbf{u}^i$ and $\mathbf{v}^i$ are known at a given instant $t_0 \in \mathrm{I}$, then for all $t > t_0$, $t \in \mathrm{I}$, the problem to be solved is the following: (where the reference to time and Lebesgue's measures symbols $\mathrm{d}\Omega_0^i$ and $\mathrm{d}\Gamma_c$ are omitted).

Find $(\mathbf{v}, \lambda; \mathbf{u}, S_u, S_v) \in \mathbf{CA}_v \times H \times \mathbf{CA}_u \times (L^\infty(\Gamma_c))^2$; $\forall (\mathbf{w}, \lambda^*) \in \mathbf{CA}_v \times H$

$$\sum_{i=1}^{2} \int_{\Omega_0^i} \rho_0^i \dot{\mathbf{v}}^i . \mathbf{w}^i + \sum_{i=1}^{2} \int_{\Omega_0^i} \mathrm{Tr}[\overline{\mathbf{\Pi}}^i (v^i)(\nabla_p(\mathbf{w}^i))^{\mathrm{T}}] - \int_{\Gamma_c} S_u S_v \lambda [\![w_n]\!] = 0 \tag{32}$$

$$-\frac{1}{h_n} \int_{\Gamma_c} [\lambda - S_u S_v (\lambda - h_n [\![v_n]\!])] \lambda^* = 0 \tag{33}$$

$$\mathbf{u}^i(t) = \mathbf{u}^i(t_0) + \int_{t_0}^{t} \mathbf{v}^i(s)\, \mathrm{d}s \quad \text{in } \Omega_0^i \tag{34}$$

$$S_u - 1_{R^-}(-d_n) = 0 \quad \text{on } \Gamma_c \tag{35}$$

$$S_v - 1_{R^-}(\lambda - \rho_n [\![v_n]\!]) = 0 \quad \text{on } \Gamma_c \tag{36}$$

where $\mathbf{CA}_v$ and $\mathbf{CA}_u$ are the spaces of kinematically admissible velocity and displacement fields, H is the space of contact Lagrange multipliers and $\overline{\mathbf{\Pi}}^i$ is given by $\overline{\mathbf{\Pi}}^i(v^i) = \mathbf{\Pi}^i(u^i)$.

As a matter of fact the system of Equations (33), with S_u and S_v defined by (35) and (36), respectively, can be splitted into two parts expressing in a weak sense a closed gap condition ($S_u S_v = 1$) or a free normal natural condition ($S_u S_v = 0$). In the former alternative, it is clear that the kinematical constraint is taken into account by means of the Lagrange multiplier λ and the formulation is a Lagrangian one. In the literature and by following pioneering works of Powell and Hestenes [37, 38] (see also [8, 9]), Alart and Curnier [10] derived an augmented Lagrangian formulation for discrete frictional contact problems (see also [2], for a variant in the continuous framework). However, as can be checked for instance in [5] or [12], there is no possibility to derive a pure Lagrangian formulation from the augmented one by simply letting the so-called augmentation parameter be equal to zero. Here we can verify that, similarly to the alternative essential boundary condition (16) established in static, in dynamic regime we have $S_u S_v [\![v_n]\!] = 0$, on Γ_c. Hence, one can add the following term to the weak equilibrium Equations (32), without perturbing the continuous problem (32)–(36):

$$\int_{\Gamma_c} S_u S_v k_n [\![v_n]\!] [\![w_n]\!] \tag{37}$$

with k_n standing for a positive possibly null parameter and it is essential to notice that the term defined above is not the classical contact penalty term.

One can now check that the obtained formulation, we call a stabilized Lagrangian formulation, extends both the Lagrangian and the augmented ones, in the following sense:

- the latter is recovered by taking $k_n = h_n = \rho_n > 0$,
- the former is obtained by taking $k_n = 0$ and $\rho_n = h_n > 0$

This unification is believed to be interesting from a practical point of view.

Remark 3

The derived formulation is called stabilized because in our numerical simulations, it was found that the main feature of the additional term (37) is a numerical stabilizing effect whenever the standard kinematical boundary conditions do not cancel rigid body motions of one of the two solids in the static or quasi-static regimes. This is the reason for which in our numerical tests, and unless a stabilization is needed, the parameter k_n was set equal to zero. Moreover it is to be noticed that, by distinguishing parameters from each others, a better conditioning could be achieved for the discrete global systems but we have not yet tested this aspect. Finally, the use of the same procedure, namely the addition of the term defined by (37) to the formulation of Simo and Laursen [2] is believed to be advantageous from a numerical stand point.

Remark 4

One should take care of the consistency of the stabilization/augmentation terms at the discrete level. Indeed, in situations where the approximation spaces for displacements and/or velocities (on contact zone) and for contact multipliers are different finite element spaces (still satisfying the Inf–Sup condition (e.g. Bathe and Brezzi [39])), one has to project the stabilization terms on the contact multiplier finite element space to ensure that no perturbation of the discrete solution of the pure Lagrangian problem is introduced via the stabilization. We refer to Section 6.4 for a numerical illustration.

4.2. Frictional Lagrangian formulations

An equivalent formulation of the *da Vinci–Amontons–Coulmb*'s laws is [36]

$$\mathbf{R}_\tau = \mu\lambda\mathbf{\Lambda} \quad \text{on } \Gamma_c \times \mathrm{I} \tag{38}$$

where

$$\mathbf{\Lambda} - P_{\mathbf{B}(0,1)}(\mathbf{\Lambda} + \rho_\tau[\![\mathbf{v}_\tau]\!]) = 0 \quad \text{if } S_u = 1 \tag{39}$$

$$\mathbf{\Lambda} = \mathbf{0} \quad \text{otherwise} \tag{40}$$

where S_u is defined by (28), μ is the friction coefficient, ρ_τ is a non-zero positive real parameter and $P_{\mathbf{B}(0,1)}$ is the orthogonal projection on the unit ball, with respect to the euclidian scalar product of R^d.

Now, by following in essence the lines developed in [6, 40] in the quasi-static regime, and by introducing the *Level-Set* like field S_f, defined by

$$S_f = 1_{B(0,1)}(\mathbf{\Lambda} + \rho_\tau[\![\mathbf{v}_\tau]\!]) \quad \text{on } \Gamma_c \times \mathrm{I} \tag{41}$$

where ρ_τ is a strictly positive real parameter, one can extend easily the previous dynamic frictionless formulation to take into account friction phenomena through the *da Vinci–Amontons–Coulomb*'s model and obtain the problem that follows.

Assuming that the displacement and velocity fields $\mathbf{u}$ and $\mathbf{v}$ are known at a given instant $t_0 \in I$, we solve, for all $t > t_0$ and $t \in \mathrm{I}$ the following problem:

Find $(\mathbf{v}, \lambda, \mathbf{\Lambda}; \mathbf{u}, S_u, S_v, S_f) \in \mathbf{CA}_v \times H \times \mathbf{H} \times \mathbf{CA}_u \times (L^\infty(\Gamma_c))^3$; $\forall (\mathbf{w}, \lambda^*, \mathbf{\Lambda}^*) \in \mathbf{CA}_v \times H \times \mathbf{H}$

$$\sum_{i=1}^{2} \int_{\Omega_0^i} \rho_0^i \dot{\mathbf{v}}^i . \mathbf{w}^i + \sum_{i=1}^{2} \int_{\Omega_0^i} \mathrm{Tr}[\overline{\mathbf{\Pi}}^i(\mathbf{v}^i)(\nabla_p(\mathbf{w}^i))^{\mathrm{T}}] - \int_{\Gamma_c} S_u S_v \lambda [\![w_n]\!]$$

$$- \int_{\Gamma_c} \mu\lambda S_u \left[S_f \mathbf{\Lambda} + (1 - S_f) \frac{\mathbf{\Lambda} + h_2^\tau [\![\mathbf{v}_\tau]\!]}{\| \mathbf{\Lambda} + h_2^\tau [\![\mathbf{v}_\tau]\!] \|} \right] [\![\mathbf{w}_\tau]\!] = 0 \tag{42}$$

$$- \frac{1}{h_n} \int_{\Gamma_c} [\lambda - S_u S_v (\lambda - h_n [\![v_n]\!])] \lambda^* = 0 \tag{43}$$

$$\int_{\Gamma_c} \left(\frac{S_f}{h_1^\tau} + \frac{1 - S_f}{h_2^\tau} \right) \mu\lambda S_u \left[\mathbf{\Lambda} - \left[S_f (\mathbf{\Lambda} + h_1^\tau [\![\mathbf{v}_\tau]\!]) \right.\right.$$

$$\left.\left. + (1 - S_f) \frac{\mathbf{\Lambda} + h_2^\tau [\![\mathbf{v}_\tau]\!]}{\| \mathbf{\Lambda} + h_2^\tau [\![\mathbf{v}_\tau]\!] \|} \right] \right] \mathbf{\Lambda}^* + \int_{\Gamma_c} (1 - S_u) \mathbf{\Lambda}\mathbf{\Lambda}^* = 0 \tag{44}$$

$$\mathbf{u}^i(t) = \mathbf{u}^i(t_0) + \int_{t_0}^{t} \mathbf{v}^i(s)\, \mathrm{d}s \quad \text{in } \Omega_0^i \tag{45}$$

$$S_u - 1_{R^-}(-d_n) = 0 \quad \text{on } \Gamma_c \times \mathrm{I} \tag{46}$$

$$S_v - 1_{R^-}(\lambda - \rho_n[\![v_n]\!]) = 0 \quad \text{on } \Gamma_c \times \mathrm{I} \tag{47}$$

$$S_f - 1_{B(0,1)}(\boldsymbol{\Lambda} + \rho_\tau[\![\mathbf{v}_\boldsymbol{\tau}]\!]) = 0 \quad \text{on } \Gamma_c \times \mathrm{I} \tag{48}$$

where $\mathbf{H}$ is the space of friction (semi-)Lagrangian multipliers and where h_2^τ and h_1^τ are a strictly positive and a non-zero real parameters, respectively.

The system of Equations (43) in which S_u, S_v, and S_f are, respectively, given by Equations (46)–(48) is a weak form of the Coulomb's friction laws. The three terms in (43) express sticking ($S_u = 1$ and $S_f = 1$), sliding ($S_u = 1$ and $S_f = 0$) and free friction state ($S_u = 0$), respectively. In sticking zones, the unknown vector valued $\boldsymbol{\Lambda}$ stands for a Lagrangian multiplier imposing that no relative sliding can occur while, in the sliding zones, this vector-valued is no more a Lagrangian multiplier, but a unit sliding direction. Observe here that when $S_u = 1$ and $S_f = 1$, the first term in the virual work of friction loads in (42) can be replaced (without perturbation) by the following more general one:

$$-\int_{\Gamma_c} \mu\lambda S_u S_f(\boldsymbol{\Lambda} + k_\tau[\![\mathbf{v}_\boldsymbol{\tau}]\!])[\![\mathbf{w}_\boldsymbol{\tau}]\!] \tag{49}$$

with $k_\tau \geqslant 0$. We recover here a possibility of stabilization similar to the one discussed in the frictionless situation.

Now, to solve the continuous and non-linear problem defined by (42)–(48), numerical schemes and numerical algorithms are needed. Our solution strategy is described in the following section.

5. SOLUTION STRATEGY

For the sake of concision, only the frictionless contact problem, defined by (32)–(36), is discretized.

5.1. Time discretization

Keeping in mind that our formulation is velocity based, we approximate the first-order derivative with respect to time (in (32)) by the Euler implicit scheme and the integral term (34) by a first-order finite difference θ-scheme. For this, we consider the interval $\mathrm{I} = [t_0, t_f]$ to be a collection of non-overlapping time sub-intervals, i.e. $\mathrm{I} = \bigcup_{k=0}^{N} [t_k, t_{k+1}]$ and we denote by $\Delta t_k = t_{k+1} - t_k$ the time step (chosen here to be constant for simplicity) and by $(.)^k$ the time discrete approximation of the field $(.)$ at time $t = t_k$. With the considerations and the notations above, we obtain the following (frictionless) semi-discretized problem:

Assuming that the displacement and velocity fields $\mathbf{u}^k$ and $\mathbf{v}^k$ are known at a given discrete instant t_k, we solve, for the discrete time $t_{k+1} = t_k + \Delta t_k$ the following problem:

Find $(\mathbf{v}^{k+1}, \lambda^{k+1}; \mathbf{u}^{k+1}, S_u^{k+1}, S_v^{k+1}) \in \mathbf{CA}_v \times H \times \mathbf{CA}_u \times (L^\infty(\Gamma_c))^2$; $\forall (\mathbf{w}, \lambda^*) \in \mathbf{CA}_v \times H$

$$\sum_{i=1}^{2} \int_{\Omega_0^i} \rho_0^i \frac{(\mathbf{v}^i)^{k+1} - (\mathbf{v}^i)^k}{\Delta t_k} . \mathbf{w}^i + \sum_{i=1}^{2} \int_{\Omega_0^i} \mathrm{Tr}[(\overline{\boldsymbol{\Pi}}^i(v^i))^{k+1} (\nabla_p(\mathbf{w}^i))^{\mathrm{T}}]$$

$$- \int_{\Gamma_c} S_u^{k+1} S_v^{k+1} \lambda^{k+1} [\![w_n]\!] = 0 \tag{50}$$

$$-\frac{1}{h_n}\int_{\Gamma_c}[\lambda^{k+1}-S_u^{k+1}S_v^{k+1}(\lambda^{k+1}-h_n[\![v_n]\!]^{k+1})]\lambda^*=0 \tag{51}$$

$$(\mathbf{u}^i)^{k+1}=(\mathbf{u}^i)^k+\Delta t_k[(1-\theta)(\mathbf{v}^i)^k+\theta(\mathbf{v}^i)^{k+1}] \quad \text{in } \Omega_0^i \tag{52}$$

$$S_u^{k+1}-1_{R^-}(-d_n^{k+1})=0 \quad \text{on } \Gamma_c \tag{53}$$

$$S_v^{k+1}-1_{R^-}(\lambda^{k+1}-\rho_n[\![v_n]\!]^{k+1})=0 \quad \text{on } \Gamma_c \tag{54}$$

where θ is a real parameter verifying a stability condition (in linear dynamics, this parameter has to verify $\theta\geqslant 0$ and $|1-\theta|\leqslant 2/\Delta t_k\omega_{\max}$, where $\omega_{\max}$ is the maximal pulsation of the mechanical system).

We notice that in (50)–(54) the reference to the dependence of the normal vector $\mathbf{n}$ with respect to time is omitted for the clarity of notation. Moreover, the approximation (52) of (34) assumes implicitly that the time meshing fits with the time irregularities (shocks). Improved procedures such as the one given by Laursen [13] are to be used if a shock time is strictly contained within a time interval $[t_k, t_{k+1}]$.

5.2. Spatial discretization

An overview of the spatial discretization of the semi-discretized problem, defined by (50)–(54), is presented here. The velocity, displacement and Lagrangian multiplier λ are approximated by means of the finite element method, while the (irregular) *Level-Sets* fields S_u and S_v are discretized by a collocation method which consists in evaluating these fields at a finite collection of points of Γ_c, the most 'appropriate' choice being the collection of numerical integration points well-suited for an accurate approximation of the integrals involving irregular contact terms. Notice here that finite element discretizations and large transformations generally lead to irregular current contact interfaces (even when the initial contact interface is plane). This relevant issue in computational contact mechanics is not developed here. We just mention that when needed we use a simple smoothing procedure based on a weighted averaging of the local frames at mesh nodes and a classical interpolation technique to create iteratively continuous normal and tangent fields to the master (numerical) contact surface (see [40], for details). For more elaborate smoothing methods, we refer to Belytschko *et al.* [41] and to the references mentioned therein.

5.2.1. FE Approximation. Let, for $i=1,2$, $\mathcal{T}_h^i$ denote a classical mesh of Ω_0^i assumed to be polygonal for $d=2$ and polyhedral for $d=3$. Let Γ_{ch} denote a mesh of Γ_c, assumed here to be constituted of edges of elements of $\mathcal{T}_h^1$. Let then $\mathbf{CA}_{vh}^i$ and H_h be classical finite element spaces, associated to $\mathbf{CA}_v^i$ and H, and $(\mathbf{w}_{L_l}^i)_{\substack{1\leqslant L\leqslant N_{lh}^i \\ l=1,d}}$, $(\psi_m)_{1\leqslant m\leqslant N_{ch}}$, respective finite element basis, with:

$$\mathbf{w}_{L_l}^i=w_L^i\mathbf{e}_l \tag{55}$$

where $\mathbf{w}_L^i$ is an element of the scalar basis generating the discrete space $(CA_{vh}^i)_l$.

By using these finite dimensional spaces, one can associate to the continuous problem, defined by (50)–(54), the following discrete system:

Find $(\mathbf{v}_h^{k+1}, \lambda_h^{k+1}; \mathbf{u}_h^{k+1}, S_u^{k+1}, S_v^{k+1}) \in \mathbf{CA}_{vh} \times H_h \times \mathbf{CA}_{uh} \times (L^\infty(\Gamma_c))^2$; $\forall (\mathbf{w}_{L_l}, \psi_m)$

$$(\mathbf{G}_{\text{dyn}})_h^{k+1} + (\mathbf{G}_{\text{int}})_h^{k+1} + (\mathbf{G}_{\text{cont}})_h^{k+1} = 0 \tag{56}$$

$$-\frac{1}{h_n} \int_{\Gamma_{ch}} [\lambda_h^{k+1} - S_u^{k+1} S_v^{k+1} (\lambda_h^{k+1} - h_n [\![v_n]\!]_h^{k+1})] \psi_m = 0 \tag{57}$$

$$(\mathbf{u}^i)_h^{k+1} = (\mathbf{u}^i)_h^k + \Delta t [(1-\theta)(\mathbf{v}^i)_h^k + \theta (\mathbf{v}^i)_h^{k+1}] \tag{58}$$

$$S_u^{k+1} - 1_{R^-}(-(d_n)_h^{k+1}) = 0 \quad \text{on } \Gamma_c \tag{59}$$

$$S_v^{k+1} - 1_{R^-}(\lambda_h^{k+1} - \rho_n [\![v_n]\!]_h^{k+1}) = 0 \quad \text{on } \Gamma_c \tag{60}$$

where

$$(\mathbf{G}_{\text{dyn}})_h^{k+1} = \sum_{i=1}^{2} \int_{\Omega_0^i} \rho_0^i \frac{(\mathbf{v}^i)_h^{k+1} - (\mathbf{v}^i)_h^k}{\Delta t} . \mathbf{w}_{L_l}^i \tag{61}$$

$$(\mathbf{G}_{\text{int}})_h^{k+1} = \sum_{i=1}^{2} \int_{\Omega_0^i} \text{Tr}[(\overline{\mathbf{\Pi}}^i)_h^{k+1} (\nabla_p (\mathbf{w}_{L_l}^i))^{\text{T}}] \tag{62}$$

$$(\mathbf{G}_{\text{cont}})_h^{k+1} = -\int_{\Gamma_{ch}} S_u^{k+1} S_v^{k+1} \lambda_h^{k+1} [\![\mathbf{w}_{L_l}]\!] . \mathbf{n} \tag{63}$$

$$(\mathbf{v}^i)_h^{k+1} = \sum_{l=1}^{d} \sum_{L=1}^{N_{lh}^i} (v_{L_l}^i)^{k+1} w_L^i . \mathbf{e}_l, \quad i = 1, 2 \tag{64}$$

$$\lambda_h^{k+1} = \sum_{m=1}^{N_{ch}} \lambda_m^{k+1} \psi_m \tag{65}$$

The problem defined above is still not completely discretized since the *Level-Sets* S_u and S_v are still not approximated. For a full discretization, we use a collocation method (a kind of finite particle approach [6, 40] or finite pointwise Dirac's measures) to approximate these irregular fields.

5.2.2. Collocation method. If $(\mathbf{p}_j)_{1 \leqslant j \leqslant N_{pc}}$ is a finite collection of points in Γ_{ch} and $S_u^{N_{pc}} = (S_u^j)_{j=1,\, N_{pc}}$, $S_v^{N_{pc}} = (S_v^j)_{j=1,\, N_{pc}}$ denote the values of S_u and S_v at points $(\mathbf{p}_j)_{j=1,\, N_{pc}}$, the complete discretization of the dynamic frictionless contact problem is achieved as follows.

Find $(\mathbf{v}_h^{k+1}, \lambda_h^{k+1}; \mathbf{u}_h^{k+1}, (S_u^{N_{pc}})^{k+1}, (S_v^{N_{pc}})^{k+1}) \in \mathbf{CA}_{vh} \times H_h \times \mathbf{CA}_{uh} \times \{0,1\}^{2N_{pc}}$; $\forall (\mathbf{w}_{L_l}, \psi_m)$

$$(\mathbf{G}_{\text{dyn}})_h^{k+1} + (\mathbf{G}_{\text{int}})_h^{k+1} - \sum_{j=1}^{N_{pc}} \omega_j (S_u^j)^{k+1} (S_v^j)^{k+1} \lambda_h^{k+1}(\mathbf{p}_j) [\![\mathbf{w}_{L_l}(\mathbf{p}_j)]\!].\mathbf{n}(\mathbf{p}_j) = 0 \tag{66}$$

$$-\frac{1}{h_n} \sum_{j=1}^{N_{pc}} \omega_j [\lambda_h^{k+1}(\mathbf{p}_j) - (S_u^j)^{k+1} (S_v^j)^{k+1} (\lambda_h^{k+1}(\mathbf{p}_j) - h_n [\![v_n]\!]_h^{k+1}(\mathbf{p}_j))] \psi_m(\mathbf{p}_j) = 0 \tag{67}$$

$$(\mathbf{u}^i)_h^{k+1} = (\mathbf{u}^i)_h^k + \Delta t[(1-\theta)(\mathbf{v}^i)_h^k + \theta(\mathbf{v}^i)_h^{k+1}] \quad \text{for } i = 1, 2 \tag{68}$$

$$(S_u^j)^{k+1} - 1_{R^-}(-(d_n)_h^{k+1}(\mathbf{p}_j)) = 0 \quad \forall j = 1, N_{pc} \tag{69}$$

$$(S_v^j)^{k+1} - 1_{R^-}(\lambda_h^{k+1}(\mathbf{p}_j) - \rho_n [\![v_n]\!]_h^{k+1}(\mathbf{p}_j)) = 0 \quad \forall j = 1, N_{pc} \tag{70}$$

with ω_j standing for a weight associated to the point $\mathbf{p}_j$, for $j = 1, N_{pc}$.

In practice, the finite element spaces $\mathbf{CA}_h^i$ and H_h have to be chosen in such a way that they fulfil the well-known LBB compatibility condition [39, 42–44]. The set of collocation contact points have also to be chosen with caution. These two issues have been discussed in the static regime in [40]. The reader is referred to this reference and to the references therein since the choices done there are those used in the dynamic framework considered here. An essential aspect shown in [40] is the importance of the refinement in terms of collocation contact points in order to obtain accurate numerical results, particularly for non-matching contact surfaces.

Remark 5
When taking into account friction phenomena, the additional friction terms are discretized by following basically the lines developed in the frictionless case.

5.3. Algorithmic development

A numerical algorithm is needed to solve the non-linear discrete contact problems defined by (66)–(70), (61)–(63). The strategy we use is based on nested loops where fixed point algorithms are combined with a Newton method (or a generalized Newton method when friction phenomena are taken into account). More precisely, at each time step, the following nested loops are considered.

- (Geometrical contact outer loop) The pairing discrete mapping and the local frames at the collocation contact points are fixed to values obtained by solving the local pairing problems (see Section 2.2) for given position of the contact interface; the initial position being the one assumed to be known at the previous time step.
- (*Level-Sets* intermediate loop) The *Level-Sets* at the collocation contact points are also assigned given values (either 0 or 1).

When the aforementioned quantities are fixed in (66)–(68), one has then to solve a non-linear finite system where the non-linearities are only due to the internal loads. For the solution of this system, a Newton method is used (this constitutes the most inner loop). At the convergence of the Newton strategy, new displacement, velocity and contact force fields are obtained. The fixed

quantities are then updated sequentially. More precisely, new *Level-Sets* are calculated by using (69), (70) and the new displacement, velocity and contact force fields. If by comparison of the new *Level-Sets* with the fixed ones, the convergence is not reached, the new *Level-Sets* are substituted to the fixed ones and a new non-linear system is solved by using the Newton method. Otherwise, the new displacement field is compared to the one used for the computation of paired points in the geometrical contact loop. If the convergence is reached, the time is incremented. Otherwise, new paired points and new local frames, evaluated at these points, are calculated, substituted to the fixed paired points and frames and used for the computation of a new solution by using the Newton method. The algorithm is stopped when all loops reach convergence.

The derivation of the linear tangent system at each iteration of the Newton's method is straightforward. It is not detailed here.

When taking into account friction phenomena, three modifications of the global algorithm described above are made. First, another nested loop is added in which the friction threshold is fixed. Second, a discrete friction *Level-Set* (S_f) is added and fixed in the *Level-Sets* loop. Third, and due to the irregularity of the sliding term (see Equation (42) or (43)), a generalized Newton method [45] is substituted to the classical Newton one. The global strategy is schematically described by Figure 2 in which the subscript k refers to the time step and the subscript g affected to a field

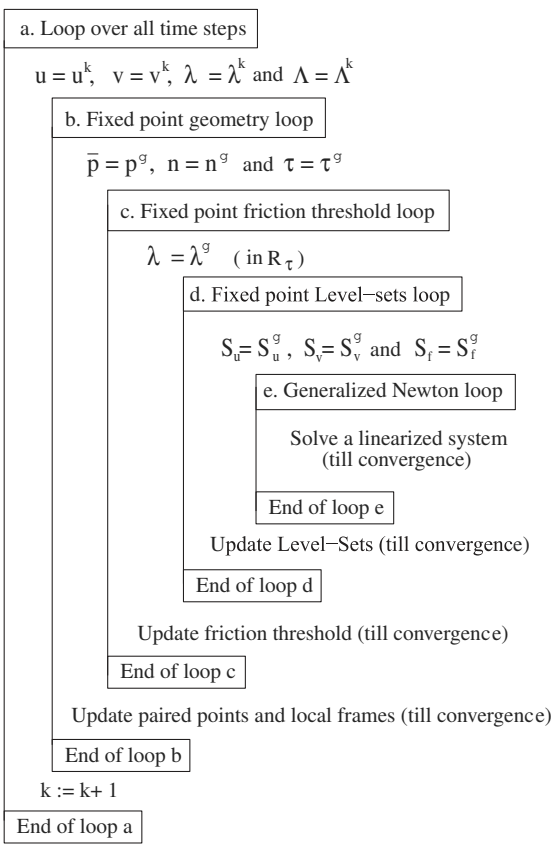

Figure 2. Global solution strategy.

means that the latter is frozen at a given value when solving each global non-linear system in the most inner loop. Actually, it is updated iteratively till reaching convergence, as explained above.

6. NUMERICAL EXAMPLES

To show the potential of our global strategy, we consider first quite academic tests: two frictionless contact-impact examples and a frictional impact one. The last example shows the numerical perturbation induced by the stabilization/augmentation term when the latter is not consistent with the discrete Lagrangian treatment of the contact (cf. Remark 4). We notice that for the three dynamic contact tests, we used our Lagrangian formulation with $\kappa_n = 0$. We have noticed no particular influence of the parameters h_n as far as it is chosen in a reasonable range. As for ρ_n, we have noticed no particular influence either. Moreover, thanks to the solution algorithm detailed in the previous section, one can easily check that, when the collocation contact points coincide with the nodes of Γ_{ch}, we can get rid of this parameter. Indeed, for this particular node-to-face treatment of contact, we have at each contact point either the contact pressure $\lambda = 0$ or the velocity jump $[\![v_n]\!] = 0$. So, in either case the updating of S_v at the *Level-Sets* loop needs no particular parameter.

6.1. Impact of two elastic rods

We consider the classical test of impact of two identical elastic prismatic rods moving with equal speed in opposite directions (Figure 3) and for which analytical solution is available [46]. The rods are initially undeformed. The initial gap is equal to 0.001 m, the velocity of the two bars is $10\ \mathrm{m\ s^{-1}}$. The mechanical properties of the two rods are: density $\rho = 7800\ \mathrm{kg\ m^{-3}}$, area of cross section $A = 4 \times 10^{-4}\ \mathrm{m^2}$, length $L = 1$ m, Young's modulus $E = 2 \times 10^{11}$ Pa and Poisson's ratio $\nu = 0.3$. We mesh the two rods similarly with Hexa 3D-elements. Bilinear finite element spaces are used to approximate the contact pressure. Three 3D-finite element solutions are plotted in Figure 4. The first one (Figure 4(a)) is obtained with a dissipative Newmark scheme ($\beta = 0.3025$, $\gamma = 0.6$) used for the time discretization of a classical displacement based Lagrangian formulation. The other solutions (cf. Figures 4(b), (c)) are obtained with our continuous velocity based formulation in which we have chosen $\theta = 1$. The time step is equal to 10^{-5} s for the first two simulations and to 2×10^{-6} s for the last one.

The results plotted in Figure 4 show that the spurious oscillations of the velocity and contact loads fields observed for the classical approach are completely treated in our approach. In addition, one can check that the refinement of the time step (Figure 4(c)), leads to more accurate results, by comparison with the known analytical solution [46]. Other schemes of the stable Newmark family have been tested for a classical displacement based Lagrangian formulation. The results always show spurious oscillations after shock instants.

6.2. Impact of a cylinder on a wall

The problem of an elastic-cylinder impacting a quasi-rigid wall under plane strain conditions is considered in this second test. Notice that when compared to the previous example, the contact zone is variable herein with respect to time. The material and geometric

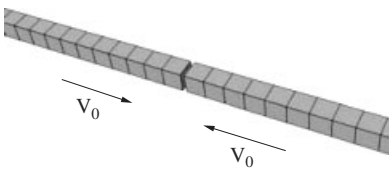

Figure 3. Impact of two 3D elastic and similar rods.

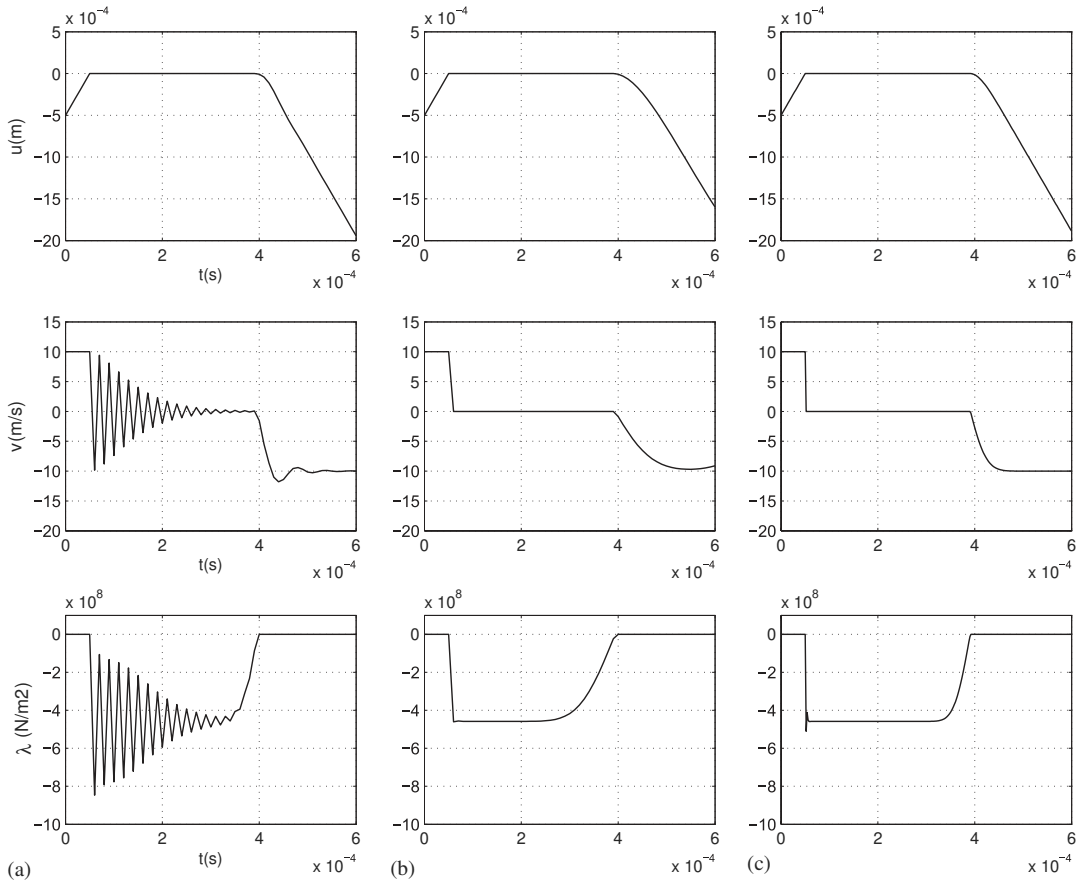

Figure 4. Impact of two identical rods: histories of tip displacement, velocity and contact pressure.

properties are:

- Cylinder: $E = 2 \times 10^{11}$ Pa, $\rho = 7800\,\mathrm{kg\,m^{-3}}$, $\nu = 0$, $R = 3 \times 10^{-2}$ m (radius)
- Wall: $E = 2 \times 10^{15}$ Pa, $\rho = 7800\,\mathrm{kg\,m^{-3}}$, $\nu = 0$.

The initial gap is equal to 10^{-2} m and the initial velocity of the cylinder is equal to $500\,\mathrm{m\,s^{-1}}$. The velocity and contact fields are approximated by bilinear finite 2D and linear 1D elements,

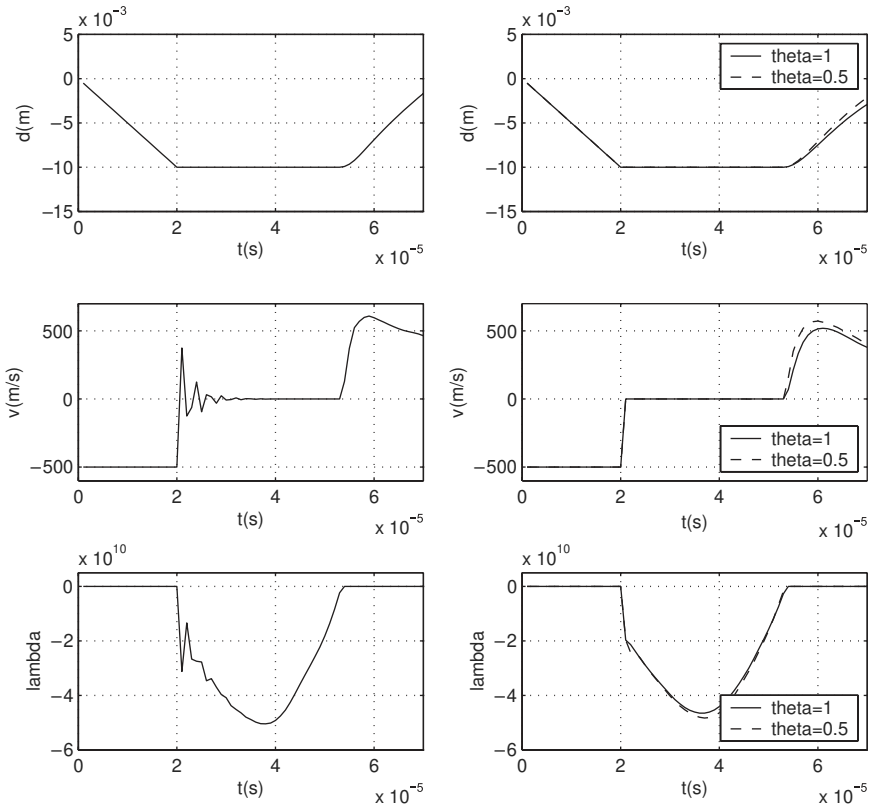

Figure 5. Impact of an elastic cylinder on a quasi-rigid wall: histories of the cylinder bottom point displacement, velocity and contact pressure.

respectively (Figure 6). The nodes of the potential slave surface (the one of the cylinder) have been taken as the collocation points for the *Level-Sets* fields. The time-step is equal to 10^{-6} s. We show in Figure 5 the time histories of the displacement, velocity and contact pressure of the bottom contacting point of the cylinder obtained by both a dissipative Newmark scheme ($\beta = 0.4$ and $\gamma = 0.7$) used for a displacement based Lagrangian formulation and the proposed method ($\theta = 1$ and 0.5). The computed deformed geometries and the stress spread in the cylinder before, during and after impact are depicted in Figure 6.

The results given by the proposed approach confirm its effectiveness to solve impact phenomena. Particularly, it does not introduce spurious oscillations. We notice that the choice of the parameter θ permits to control the numerical dissipation of the first-order time scheme during the separation phase.

6.3. Impact of Taylor's rod

This example involves the elastic–plastic impact of a rod ($E = 1.17 \times 10^5$ MPa, $v = 0.35$, $\rho = 8930$ kg m^{-3}, $\sigma_y = 400$ MPa, $E_t = 100$ MPa) against a rigid wall. The rod has an initial velocity of 227 m s^{-1}. Two cases have been performed: a frictionless and a frictional impact. For the

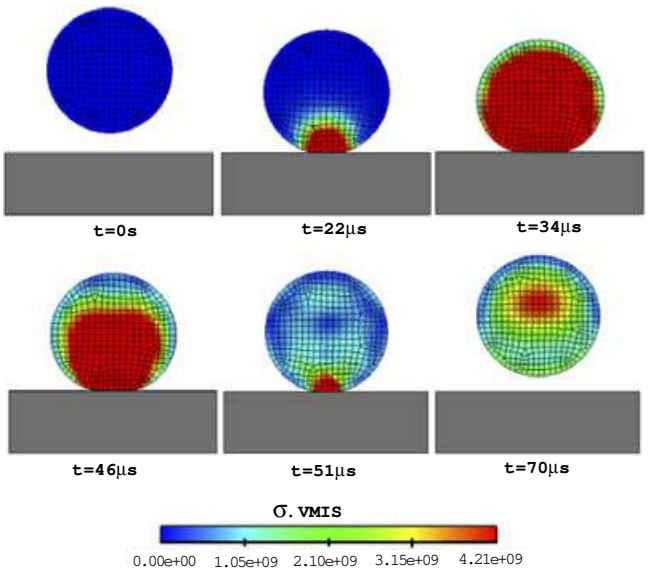

Figure 6. Computed deformed geometries and stress spread in the cylinder.

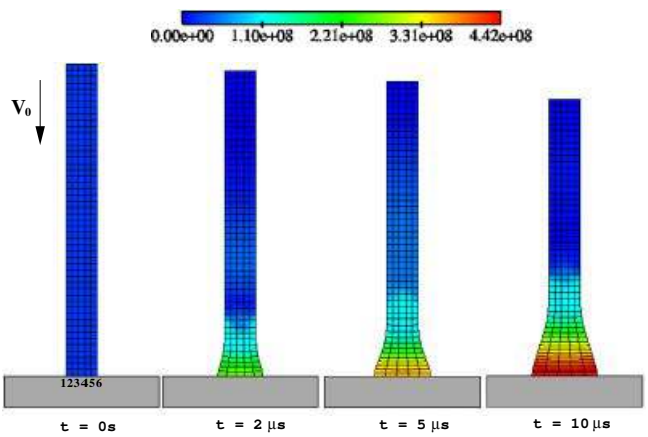

Figure 7. Frictionless elastic–plastic bar impact: Von Mises isovalues.

second case, we consider the classical Coulomb model of friction with $\mu = 0.25$. The dynamic behaviour of the rod is integrated within our global strategy, with a time step equal to 2×10^{-7} s and with bilinear finite elements used to approximate all the fields of the plane strain model of the rod.

We compare in Figure 8 the time histories of the displacement, velocity and contact pressure at point number 3 (see left part of Figure 7) obtained with (i) the classical displacement based

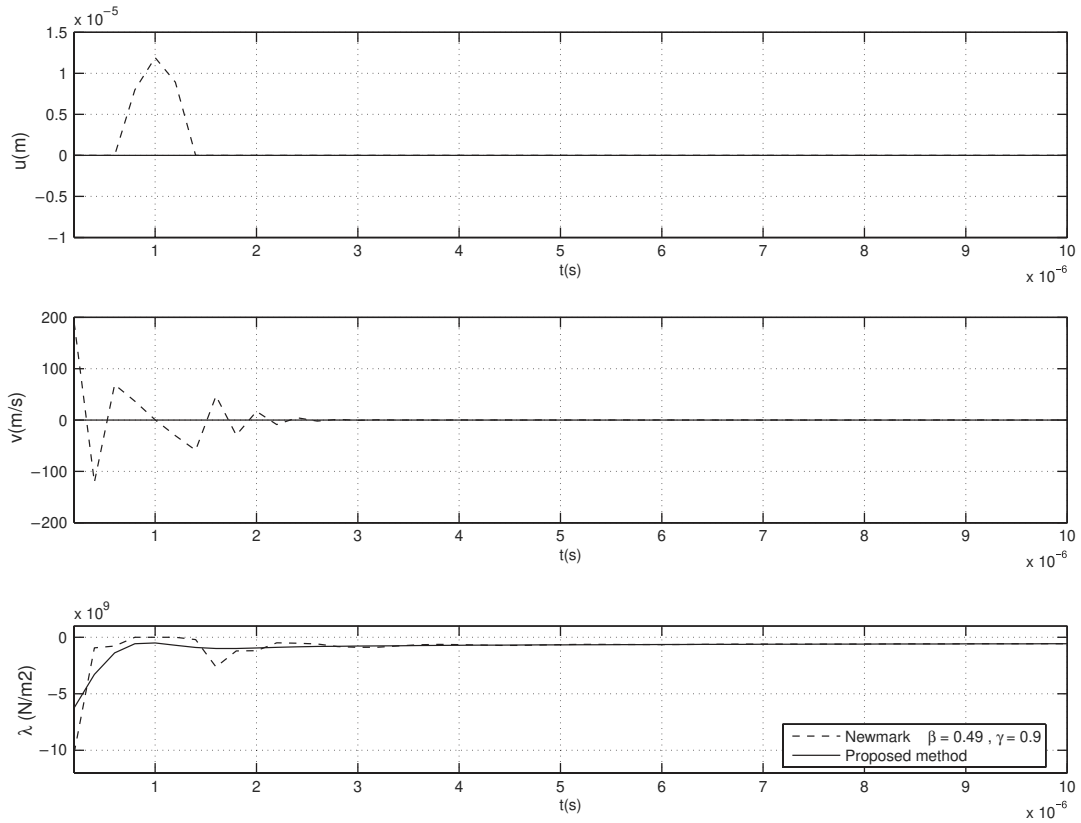

Figure 8. Frictionless elastic–plastic bar impact: displacement, velocity and contact pressure histories at point number 3 of Figure 9.

Lagrangian formulation and a dissipative Newmark scheme with $\beta = 0.49$ and $\gamma = 0.9$ (dashed lines) and (ii) our approach with $\theta = 1$ (solid lines). These results show that the present approach is more robust. Particularly, we obtain no oscillations on displacement and velocity fields. Moreover, the profile of contact multipliers is more regular, when compared to the one given by the first method. Notice that the normal gap d_n and velocity jump $[\![v_n]\!]$ between contact points are equal to zero, which means that the *Signorini-Moreau* conditions are perfectly respected.

We show also in Figure 7 (frictionless impact) and Figure 9 (frictional impact) the deformed geometries and the Von-Mises stress spread in the Taylor's rod at three selected instants during the impact.

The time histories of the Lagrangian semi-multiplier of friction $\mathbf{\Lambda}$ at the six nodes of the (slave) contact surface (cf. left part of Figure 9) are depicted in Figure 10. The values of this field indicate the states of contact points: a contact point is sticking when $\|\mathbf{\Lambda}\| < 1$ and sliding when $\|\mathbf{\Lambda}\| = 1$.

Figure 11 depicts the deformed geometries of the Taylor's rod when our impact finite element model is refined. Notice that the classical rising up of the contact edge in frictionless contact case is retrieved (Figure 11(a)).

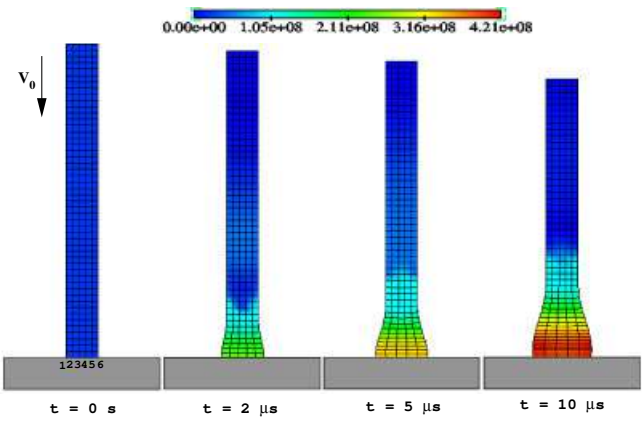

Figure 9. Frictional elastic–plastic bar impact: Von Mises isovalues.

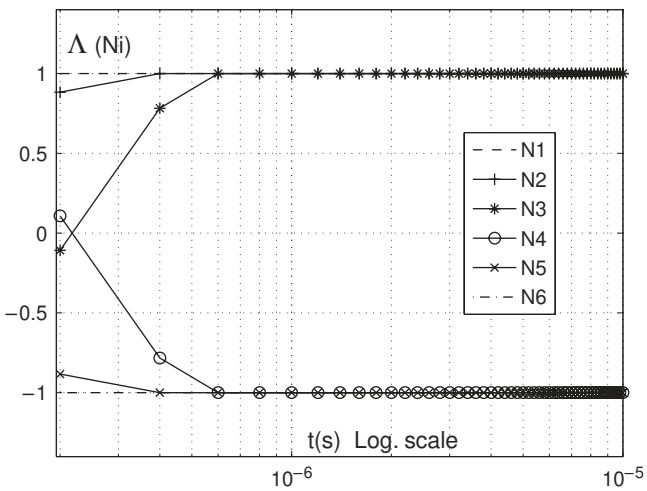

Figure 10. Frictional elastic–plastic bar impact: semi-Lagrangian friction multiplier histories at contact points.

6.4. Consistency stabilization test

The point of focus of this test is the consistency of the stabilization/augmentation terms at the discrete level (cf. Remark 4). We consider the simple frictionless contact patch-test [47] where the two solids are meshed with non-matching meshes (Figure 12). For purpose of clear illustration, the displacements on contact zone and the contact multiplier are approximated with piece-wise linear P_1 and piece-wise constant P_0 finite elements, respectively. It is important to notice here that with these choices of the finite element spaces, the non-interpenetration of the two solids though treated with a Lagrange multiplier technique, is only satisfied in a weak and averaged sense on each element of the slave surface.

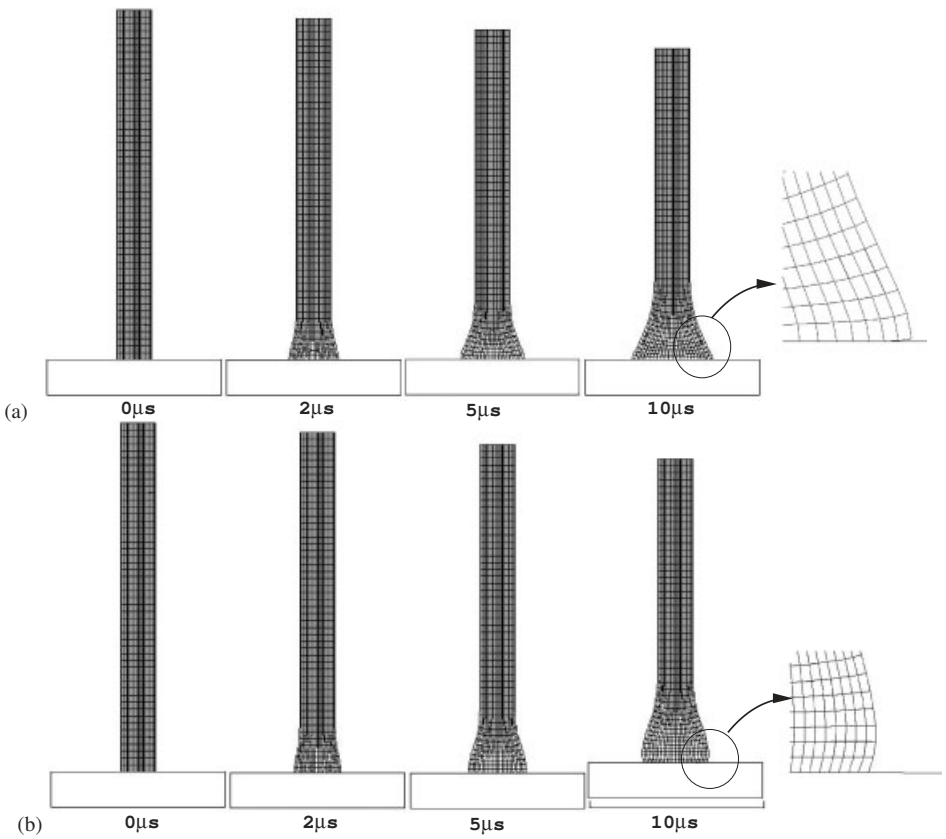

Figure 11. Frictionless and frictional elastic–plastic bar impact: refined finite element models.

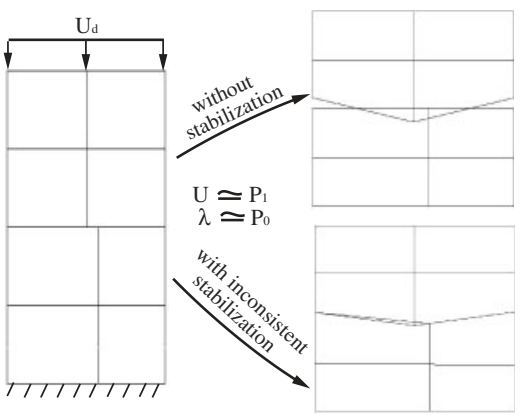

Figure 12. Patch-test without and with inconsistent stabilization.

The numerical solutions are computed with (inconsistent) and without stabilization. We notice that the inconsistent stabilization term, without projection as suggested in Remark 4, induces a perturbation of the numerical solution of the problem without stabilization (see Figure 12).

Remark 6
Notice that when the stabilized Lagrangian formulation is approximated by mortar finite elements, it may also be necessary to use the procedure described in Remark 4 near the contact edges in order not to perturb the contact numerical results.

7. CONCLUDING REMARKS

A velocity and *Sign*-like fields continuous and mixed formulation of dynamic frictional contact problems has been developed in this paper. The introduction of the *Sign* fields as fundamental and intrinsic contact unknown fields not only clarifies the difficulty related to the contact non-linearities but allows also for the derivation of a *stabilized* Lagrangian formulation, generalizing the Lagrangian and augmented Lagrangian formulations. The continuous problem is discretized by means of time, space and collocation schemes and a numerical algorithm is used for the solution of the non-linear and irregular discrete systems. Several numerical examples show the effectiveness of our approach, particularly for the treatment of the pathology related to the spurious numerical oscillations. Many other points are now being developed. Let us mention the coupling of implicit low-order schemes used in the vicinity of impact regions with explicit higher-order ones far from these critical zones in order to treat the local irregular behaviour and to prevent global dispersion phenomena. Let us also mention the superposition in the Arlequin framework [48–51] of a very fine model near the impact zone to an underlying coarser one.

ACKNOWLEDGEMENT

The support of Électricité de France is gratefully acknowledged.

REFERENCES

1. Sethian JA. *Level-Set Methods Envolving Interfaces in Geometry*, *Fluid Mechanics*, *Computer Vision and Materials Science*. Cambridge University Press: Cambridge, MA, 1996.
2. Simo JC, Laursen TA. An augmented Lagrangian treatment of contact problems involving friction. *Computers and Structures* 1992; **42**:97–116.
3. Klarbring A. Large displacement frictional contact: a continuum framework for finite element discretization. *European Journal of Mechanics – A/Solids* 1995; **2**:237–253.
4. Curnier A, He Q-Ch, Klarbring A. Continuum mechanics modelling of large deformation contact wit friction. *Contact Mechanics* 1995; **7**:145–158.
5. Pietrzak G, Curnier A. Large deformation frictional contact mechanics: continuum formulation and augmented Lagrangian treatment. *Computer Methods in Applied Mechanics and Engineering* 1999; **177**:351–381.
6. Ben Dhia H, Vautier I, Zarroug M. Problèmes de contact frottant en grandes transformations: du continu au discret. *Revue Européenne des Eléments Finis* 2000; **9**:243–261.
7. Jones RE, Papadopoulos P. A yield-limited Lagrange multiplier formulation for frictional contact. *International Journal for Numerical Methods in Engineering* 2000; **48**:1127–1149.
8. Rockafellar RT. Augmented Lagrangians and applications of the proximal point algorithm in convex programming. *Mathematics of Operations Research* 1976; **1**:97–116.

9. Fortin M. Minimization of some non-differentiable functionals by the augmented Lagrangian method of Hestenes and Powell. *Applied Mathematics and Optimization* 1976; **2**:236–250.
10. Alart P, Curnier A. A mixed formulation for frictional contact problems prone to Newton like solution methods. *Computer Methods in Applied Mechanics and Engineering* 1991; **92**:353–375.
11. De Saxcé G, Feng ZQ. New inequality and functional for contact with friction: the implicit standard material approach. *Mechanical Structures and Machines* 1991; **19**:301–325.
12. Wriggers P. *Computational Contact Mechanics*. Wiley: New York, 2002.
13. Laursen TA. *Computational Contact and Impact Mechanics*: *Fundamentals of Modeling Interfacial Phenomena in Nonlinear Finite Element Analysis*. Springer-Verlag: Heidelberg, 2002.
14. Hughes TJR, Taylor RL, Sackman JL, Curnier A, Wanoknukulchai W. A finite element method for a class of contact-impact problems. *Computer Methods in Applied Mechanics and Engineering* 1976; **8**:249–276.
15. Taylor RL, Papadopoulos P. On a finite element method for dynamic contact/impact problems. *International Journal for Numerical Methods in Engineering* 1993; **36**:2123–2140.
16. Belytschko T, Neal MO. Contact-impact by the pinball algorithm with penalty and Lagrangian methods. *International Journal for Numerical Methods in Engineering* 1991; **31**:547–572.
17. Carpenter NJ, Taylor RL, Katona MG, Lagrange constraints for transient finite element surface contact. *International Journal for Numerical Methods in Engineering* 1991; **32**:103–128.
18. Simo JC, Tarnow N. The discrete energy-momentum method. Part I. Conserving algorithms for non linear elastodynamics. *Zeitschrift fuer Angewandte Mathematik und Physik* 1992; **43**:757–793.
19. Armero F, Petocz E. Formulation and analysis of conserving algorithms for frictionless dynamic contact-impact problems. *Computer Methods in Applied Mechanics and Engineering* 1998; **158**:269–300.
20. Armero F, Petocz E. A new dissipative time-stepping algorithm for frictional contact problems: formulation and analysis. *Computer Methods in Applied Mechanics and Engineering* 1999; **179**:151–178.
21. Laursen TA, Chawla V. Design of energy conserving algorithms for frictionless dynamic contact problems. *International Journal for Numerical Methods in Engineering* 1997; **40**:863–886.
22. Laursen TA, Love GR. Improved implicit integrators for transient impact problems—geometric admissibility within the conserving framework. *International Journal for Numerical Methods in Engineering* 2002; **53**:245–274.
23. Love GR, Laursen TA. Improved implicit integrators for transient impact problems—dynamic frictional dissipation within an admissible conserving framework. *Computer Methods in Applied Mechanics and Engineering* 2003; **192**:2223–2248.
24. Moreau JJ. Unilateral contact and dry friction in finite freedom dynamics. *Nonsmooth Mechanics and Application*. CISM Courses and Lectures, vol. 302. Springer-Verlag: Wien/New York, 1988; 1–82.
25. Moreau JJ. Some numerical methods in multibody dynamics: application to granular materials. *European Journal of Mechanics – A/Solids* 1994; **13**:93–114.
26. Jean M. The non-smooth contact dynamics method. *Computer Methods in Applied Mechanics and Engineering* 1999; **177**:235–257.
27. Christensen PW, Klarbring A. Newton's methods for frictional contact problems. *CD Proceedings of First European Congress on Computational Mechanics*, Muenchen, Germany, 1999.
28. Curnier A, Alart P. A generalized newton method for contact problems with friction. *Journal de Mécanique Théorique et Appliquée* 1988; **7**:67–82.
29. Ben Dhia H, Durville D. An implicit method based on enriched kinematical thin plate model for sheet metal forming simulation. *Journal of Materials Processing Technology* 1995; **50**:70–80.
30. Ben Dhia H. Modelling and solution by panalty-duality method of unilateral contact problems. *Calcul des Structures et Intelligence Artificielle* 1988; **2**:1–18.
31. Chaudhary A, Bathe KJ. A solution for static and dynamic analysis of three-dimensional contact problems with friction. *Computers and Structures* 1986; **39**:721–739.
32. Vola D, Pratt E, Jean M, Raous M. Consistent time discretization for a dynamic frictional contact problem and complementary techniques. *Revue Européenne des Eléments Finis* 1998; **7**:149–162.
33. Ben Dhia H, Zammali C. Level-Sets and Arlequin framework for dynamic contact problems. *Revue Européenne des Eléments Finis* 2004; **13**:403–414.
34. Moreau JJ. Contact and friction in the dynamics of rigid body system. *Revue Européenne des Eléments Finis* 2000; **9**:9–28.
35. Oden JT, Martins JAC. Models and computational methods for dynamic friction phenomena. *Computer Methods in Applied Mechanics and Engineering* 1985; **52**:527–634.
36. Ben Dhia H. Modelling and numerical approach of contact and dry friction in simulation of sheet metal forming. *World Congress on Computational Mechanics* 1990; **WCCM II**:779–782.

37. Powell BT. A method for nonlinear constraints in minimization problems. In *Optimisation*, Fletchar R (ed.). Academic Press: London, 1969; 283–298.
38. Hestenes M. Multiplier and gradient methods. *Journal of Optimization Theory and Applications* 1969; **4**:303–320.
39. Bathe KL, Brezzi F. Stability of finite element mixed interpolations for contact problems. *Rendiconti Lincei*, *Mathematica eE Applicazioni*, *Ser. 9* 2001; **12**:167–183.
40. Ben Dhia H, Zarroug M. Hybrid frictional contact particles-in elements. *Revue Européenne des Eléments Finis* 2002; **9**:417–430.
41. Belytschko T, Daniel WJT, Ventura G. A monolithic smoothing-gap algorithm for contact-impact based on the signed distance function. *International Journal for Numerical Methods in Engineering* 2002; **55**:101–125.
42. Kikuchi N, Oden JT. *Contact Problems in Elasticity*: *A Study of Variational Inequalities and Finite Element Methods*. SIAM: Philadelphia, 1988.
43. Ben Belgacem F, Hild P, Laborde P. Extensions of the mortar finite element method to a variational inequality modelling unilateral contact. *Mathematical Methods in the Applied Sciences* 1999; **9**:287–303.
44. El-Abbassi N, Bathe KL. Stability and patch test performance of contact discretizations and a new solution algorithm. *Computers and Structures* 2001; **79**:1473–1486.
45. Clark FH. *Optimization and Nonsmooth Analysis*. Wiley: New York, 1983.
46. Goldsmith W. *Impact*: *The Theory and Physical Behaviour of Colliding Solids*. Edwarld Arnold: London, 1960.
47. Taylor RL, Papadopoulos P. A patch test for contact problems in two dimensions. In *Nonlinear Computational Mechanics*, Wriggers P, Wagner W (eds). Springer: Berlin, 1991; 690–702.
48. Ben Dhia H. Multiscale mechanical problems: the Arlequin method. *Comptes Rendus de l'Académie des Sciences série IIb* 1998; **326**:899–904.
49. Ben Dhia H, Zarroug M. Contact in the Arlequin framework. In *Contact Mechanics*, Martins JAC, Monteiro Marques MDP (eds). Kluwer Academic Publishers: Dordrecht, 2001; 401–410.
50. Ben Dhia H, Rateau G. The Arlequin method as a flexible engineering design tool. *International Journal for Numerical Methods in Engineering* 2005; **62**:1442–1462.
51. Ben Dhia H, Zammali C. Multiscale analysis of impacted structures. *CD Proceedings of the Fifth International Conference on Computation of Shell and Spatial Structures*, Slazburg, Austria, 2005.